	Experiment title: **High-Resolution Powder XRD Study of Composite Single Crystals**	**Experiment number:** **CH-5688**
ESRF		
Beamline: ID22	**Date of experiment:** from: 29th Oct. 2020 to: 1st Nov. 2020	**Date of report:** 05/03/2021
Shifts: 7	**Local contacts:** Ola Grendal & Catherine Dejoie	
Names and affiliations of applicants: **Principal Investigator:** Prof. Fiona Meldrum, University of Leeds **Experiment Team:** Ouassef Nahi, University of Leeds Dr. Cedrick O'Shaughnessy, University of Leeds		

Names and affiliations of applicants:

Principal Investigator: Prof. Fiona Meldrum, University of Leeds

Experiment Team: Ouassef Nahi, University of Leeds
Dr. Cedrick O'Shaughnessy, University of Leeds

1. Abstract

The synthesis of inorganic materials with nanocomposite structures – where inorganic nanoparticles are dispersed throughout an inorganic host – promises the ability to create materials with new properties, where these can be tuned according to their compositions and structures. However, traditional synthesis routes typically lead to low loadings, and aggregation of the nanoparticles. We have successfully developed a novel, facile strategy that enables the incorporation of gold nanoparticles at unprecedented levels – up to 40 wt% – and without aggregation, within single crystals. To- date, this strategy has been applied to calcite ($CaCO_3$), $MnCO_3$ and ZnO (Figure 1). We have recently discovered that further control over the structures of these nanocomposite crystals can be achieved through post- synthesis annealing. Remarkably, the gold nanoparticles grow in size without any observable structural change or loss of perfection in the host single crystal. Further, the size and separation of the gold nanoparticles can be tuned by selecting the heating rate and annealing temperature (Figure 2). This provides a highly effective means of controlling the optical properties of these unique nanocomposites – including the surface plasmon resonance and photoluminescence.
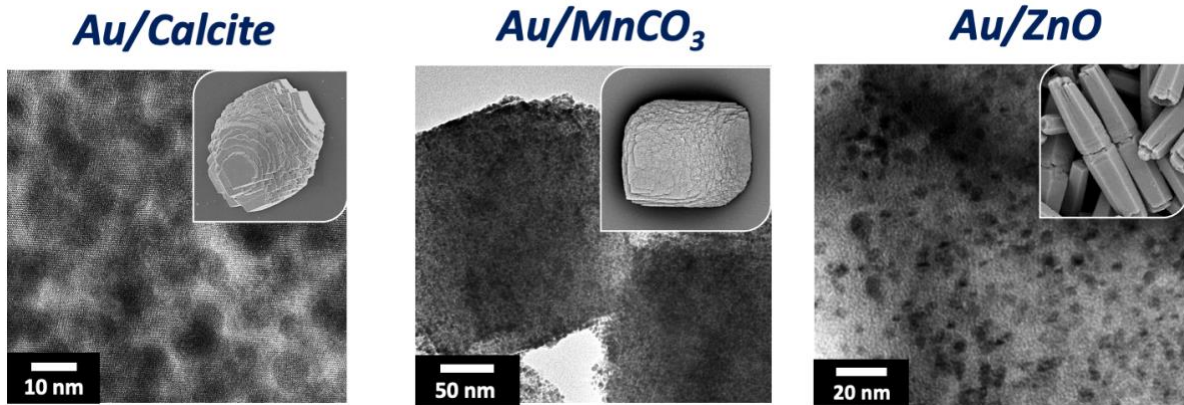
Figure 1. Transmission electron microscopy of gold nanoparticles (Au) incorporated in calcite (Au/Calcite), manganese carbonate (Au/MnCO$_3$) and zinc oxide (Au/ZnO) single crystals. Insets are scanning electron micrographs of the composite crystals.
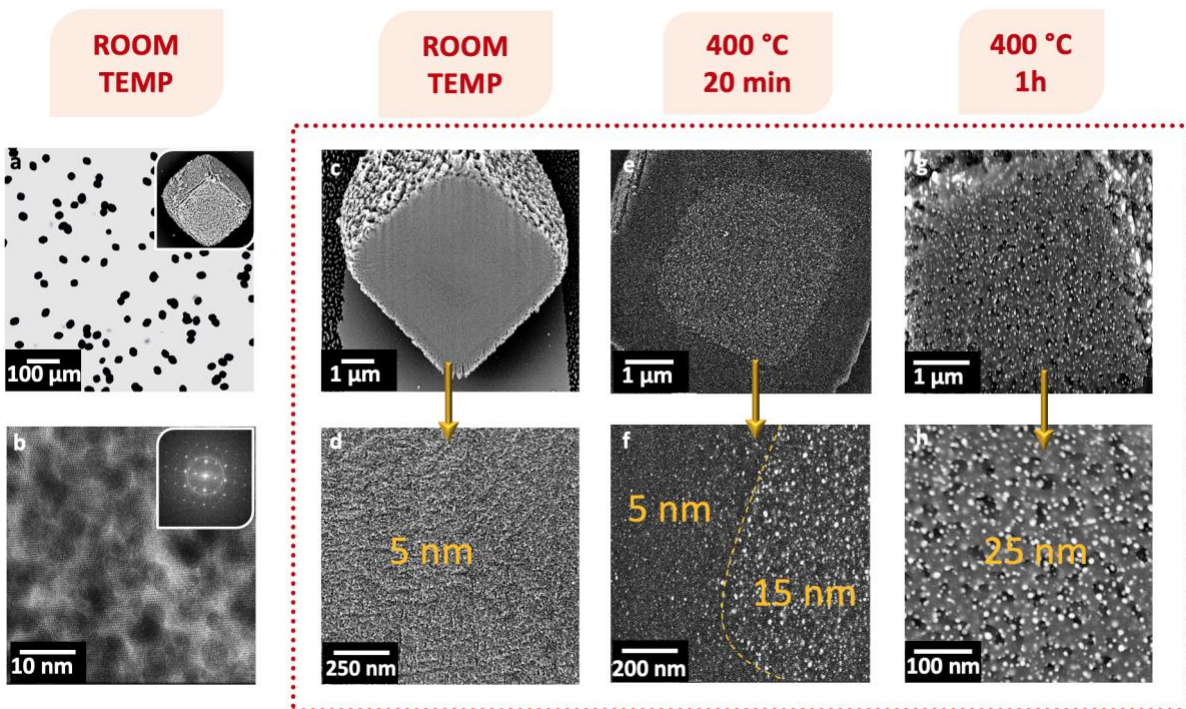

Figure 2. Optical microscope image of Au-calcite composites (a) and TEM image of the composite material (b). FIB-SEM of a cross-section of the Au-calcite composites heated at 400 °C for various time periods, showing the controlled sintering of the gold particles (c-h).

2. Experimental details

The high-resolution powder X-ray diffraction (HR-PXRD) measurements were carried out on beamline ID22 at the European Synchrotron Research Facility (ESRF), Grenoble, France, at a

wavelength of 0.35449587 ± 0.00000467 Å. Pure $CaCO_3$, $MnCO_3$ and ZnO single crystals, crystals incorporating poly(ethylene imine) (PEI) polymer and crystals embedding 5 nm gold nanoparticles functionalized with PEI (Au/PEI) were analyzed using synchrotron HR-PXRD. Samples were prepared and prior-loaded into borosilicate glass capillaries. $CaCO_3$, $MnCO_3$ and ZnO crystals were analyzed (1) at room temperature and (2) following isochronous annealing using a hot-air blower at 200 °C and 400 °C for 2 h. The diffraction patterns were analysed by Rietveld refinements using PANalytical X'Pert HighScore Plus software to provide structural details (lattice spacings, coherence lengths and microstrains). Line profile analysis were used to model the peak shapes for accurate determination of the lattice microstrains in different crystallographic directions, and to obtain information about coherence lengths.

3. Results

a. Room temperature HR-PXRD

i. Au/Calcite composites

Incorporation of polymer functionalized-gold particles (Au-PEI) within calcite single crystals yielded significant microstructural changes of the mineral host, where both a shift and a broadening of the (012), (104), (006) and (110) main diffraction peaks can be observed (Figure 3). A similar trend is also observed when only the polymer was incorporated within calcite. However, broadenings and shifts of the peaks were lesser than when Au-PEI were incorporated in calcite, demonstrating that incorporation of particulate additives functionalized with polymers yields further microstructural changes of the host crystal.
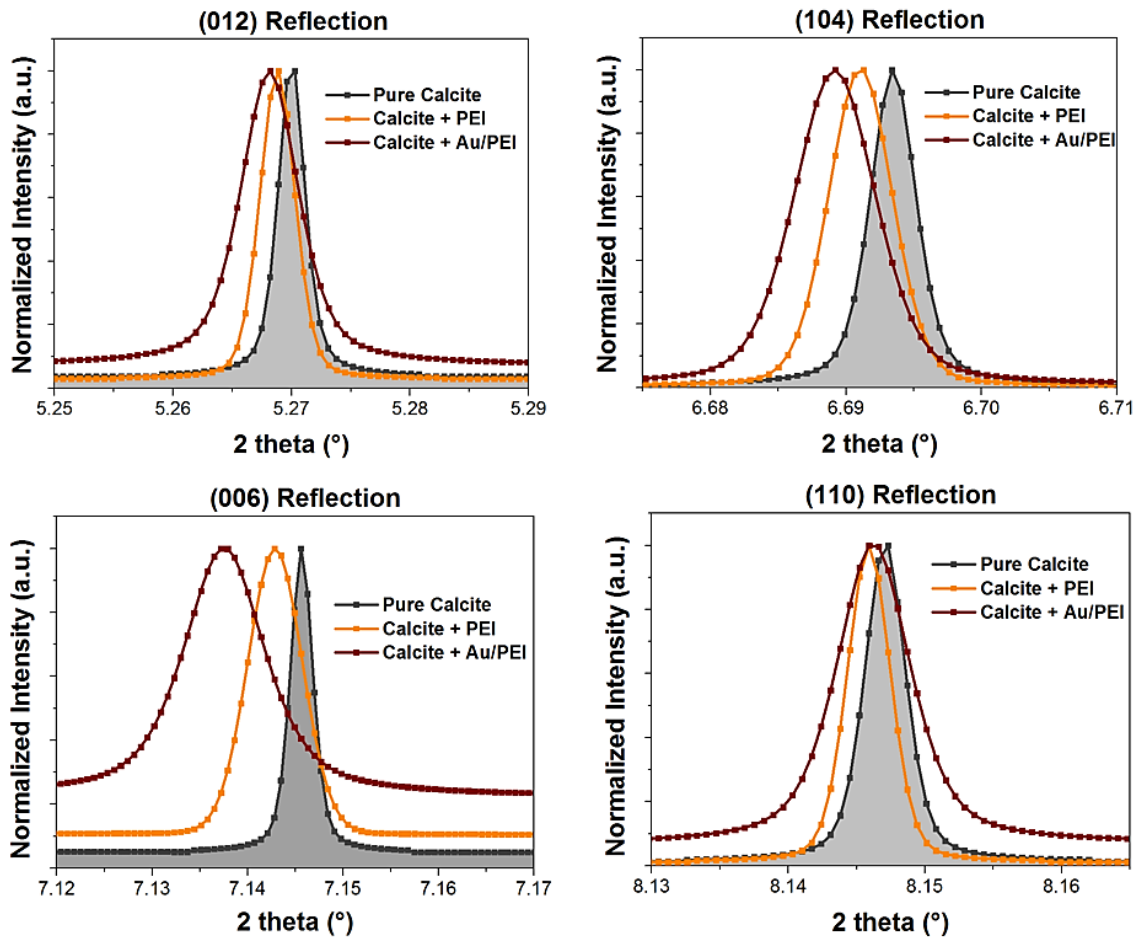
Figure 3. Graphs of the (012), (104), (006) and (110) main reflections of pure calcite (black), PEI/Calcite composites (orange) and Au/PEI incorporated in calcite (red).

Additionally, the composite crystals also displayed smaller coherence lengths and higher microstrain fluctuations than those of pure calcite, further demonstrating their efficient incorporation within the lattice of calcite (Figure 4). Furthermore, all reflections were considerably shifted towards larger d-spacings, indicating a lattice expansion of the crystals in all directions.[1] Lattice distortions that were greater along the c-axis than along the a-axis were recorded for both PEI polymer and Au-PEI (Figure 4), which is consistent with the elastic anisotropy of calcite.[1] Notably, the Au-PEI incorporated in calcite yielded lattice expansions reaching up to $\Delta c/c$ = 0.13 %. This is rather high for brittle ceramics and compares to that observed in biominerals.[2, 3]
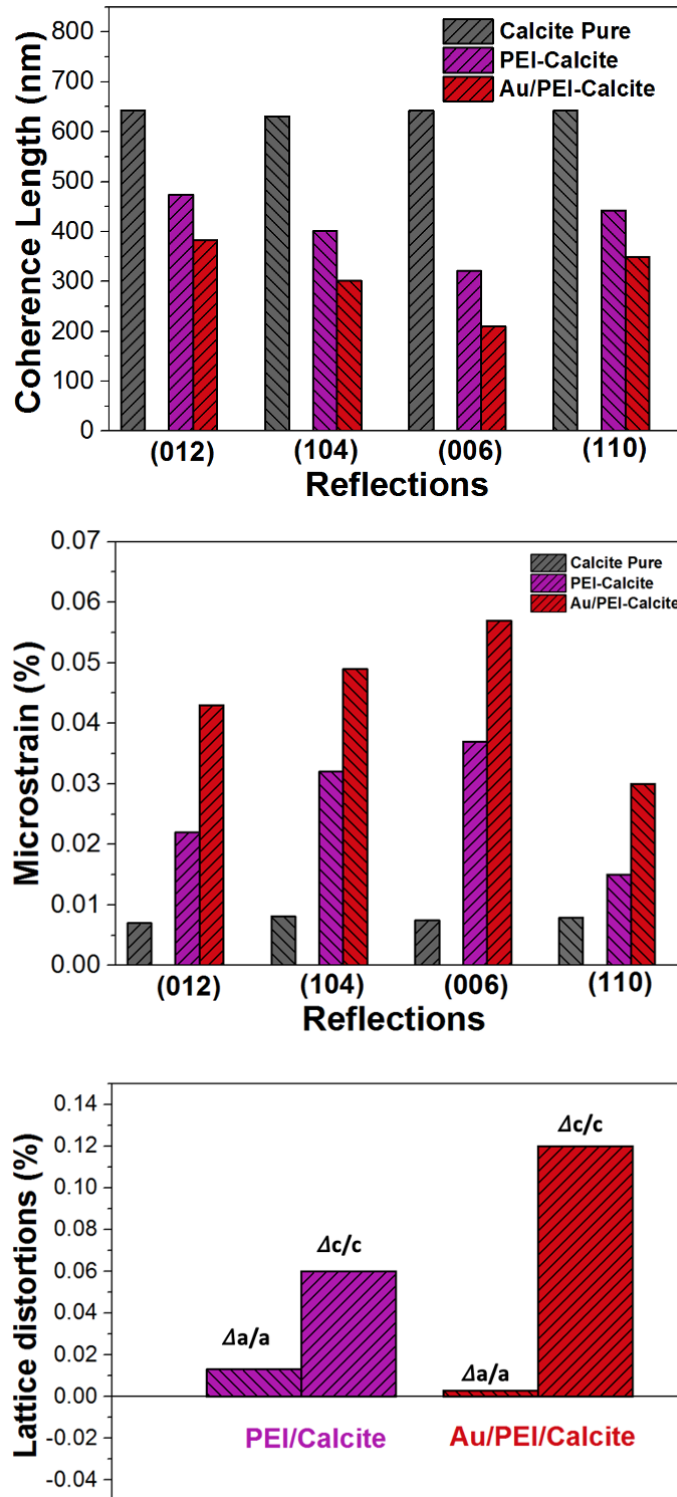
Figure 4. Coherence lengths and microstrain fluctuations of pure calcite (grey), PEI/calcite (purple) and Au/PEI/calcite (red). Bottom graph represents the lattice distortions along the a-axis and c-axis for PEI/calcite (purple) and Au/PEI/calcite (red).

ii. Au/MnCO₃ composites

We then investigated the effect of the incorporation of Au-PEI on the microstructure of the MnCO₃ (rhodochrosite) host crystal. MnCO₃ is isostructural to calcite and therefore should behave similarly to calcite when additives/impurities are incorporated within the host crystal. Surprisingly, however, incorporation of Au-PEI within MnCO₃ yielded a completely different behavior than that observed for calcite. Indeed, a shift of the diffraction peaks towards higher angles (*i.e.,* smaller d-spacings) were recorded (Figure 5). This is observed for the (012) and (104) main reflections of MnCO₃. This is somewhat counter-intuitive, as incorporation of impurities/additives usually shifts the diffractions peaks towards higher d-spacing, corresponding to a lattice expansion of the host crystals, necessary to accommodate foreign species within their lattice.[1, 4] Here, we observe, for the first-time, the lattice contraction of the rhodochrosite host crystal on incorporation of high amounts of Au-PEI guest species. Additionally, all diffractions peaks were significantly broader than pure MnCO₃, as a result of the efficient incorporation of high amounts of Au-PEI within the mineral lattice.
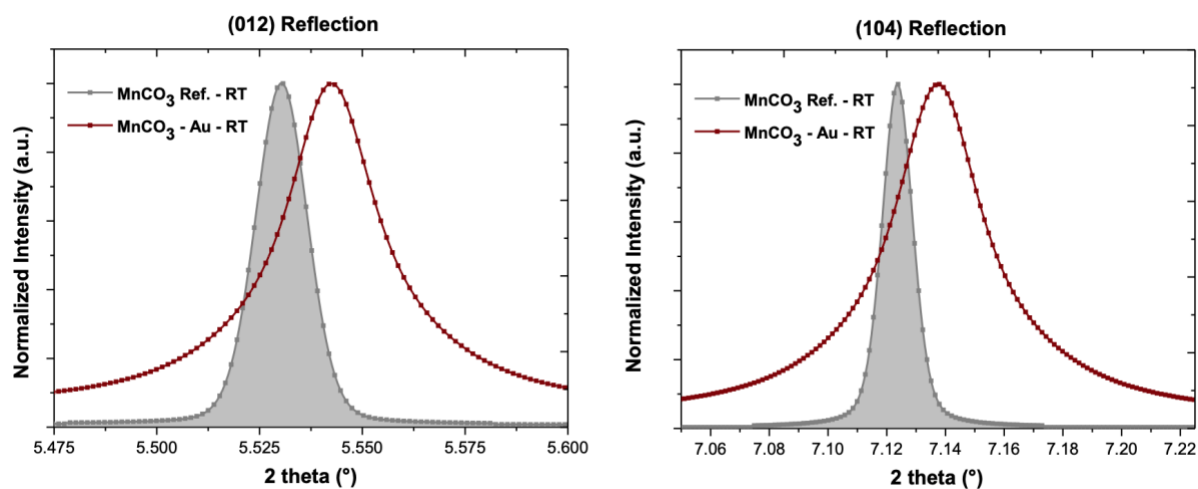

Figure 5. Graphs of the (012) and (104) main reflections of pure MnCO₃ (grey) and Au/PEI incorporated in MnCO₃ (red).

iii. Au/ZnO composites

We extended our approach to another model system, where we incorporated high levels of Au-PEI within ZnO (zincite) host crystals grown using mild-hydrothermal conditions (90 °C). Compared to pure ZnO, the Au-ZnO composite crystals displayed all main (100), (002) and (101) reflections that were shifted towards lower 2θ (*i.e.,* larger d-spacings), corresponding

to a lattice expansion of the host crystals (Figure 6). This is a similar behavior than that observed for the Au-calcite composite crystals and is indicative of efficient incorporation of the gold nanoparticles within the mineral host. More interestingly, the composites incorporating Au-PEI yielded a unique behavior, where we observed that all diffraction peaks of the ZnO host become sharper compared to pure ZnO (Figure 6). This corresponds to an increase of the coherence length and decrease of the microstrain fluctuation. That the diffractions peaks become sharper on incorporation could arise from the slower growth rate of the ZnO crystals when in the presence of Au-PEI in the precipitation solution. Indeed, it is well known that introduction of impurities/additives in the crystallization solution often slows down the rate of propagation of the steps on the mineral surface. This could allow the mineral to grow slower and therefore accumulate less defects within its crystalline structure.
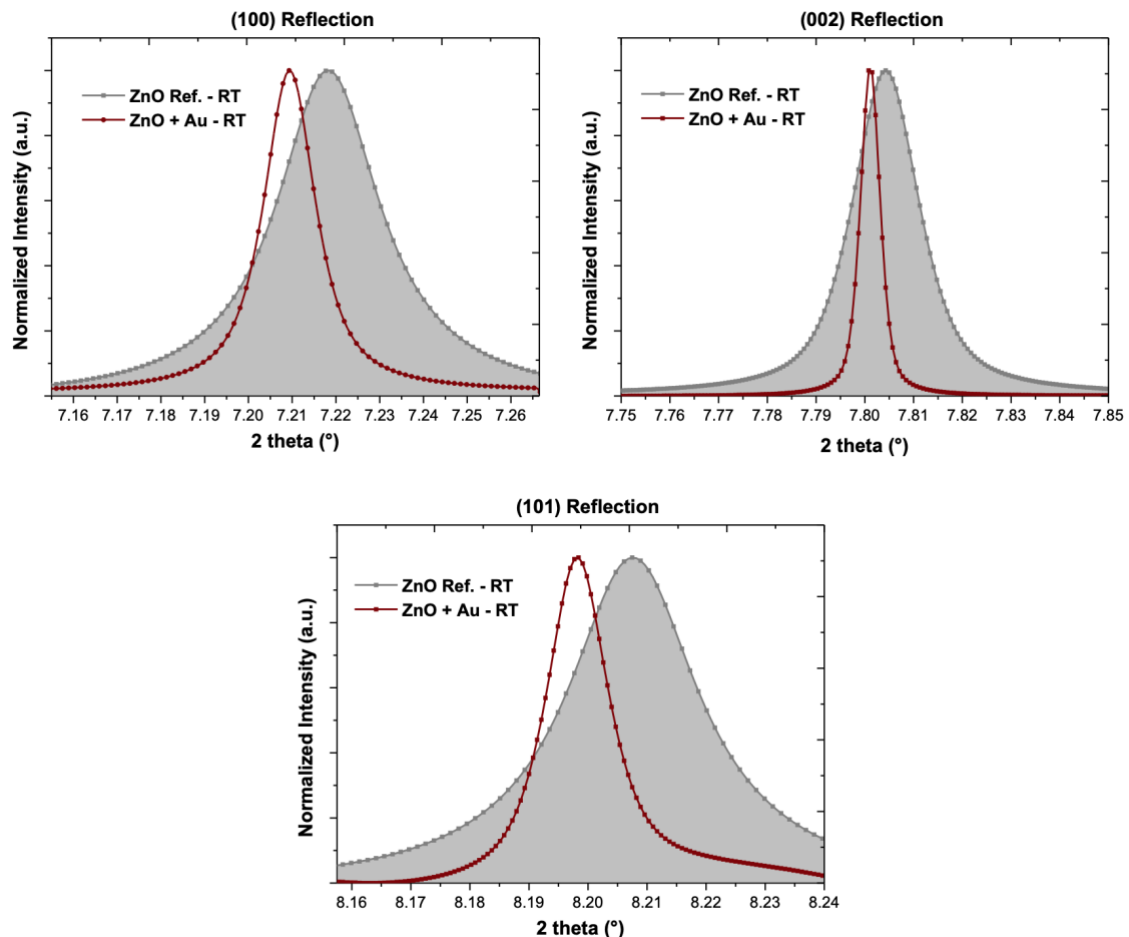

Figure 6. Graphs of the (100), (002) and (101) main reflections of pure ZnO (grey) and Au/PEI incorporated in ZnO (red).

b. Isochronous annealing of Au/Calcite composites

We then preformed isochronous annealing measurements at 200 °C and 400 °C for 2 h of the pure calcite crystals and calcite composite crystals incorporating high levels of Au-PEI nanoparticles. Annealing of pure calcite did not alter the crystal microstructure. No changes of the peaks shape, broadening or position were recorded for any of the calcite reflections (Figure 7). This demonstrates that our calcite crystals have a high purity level.
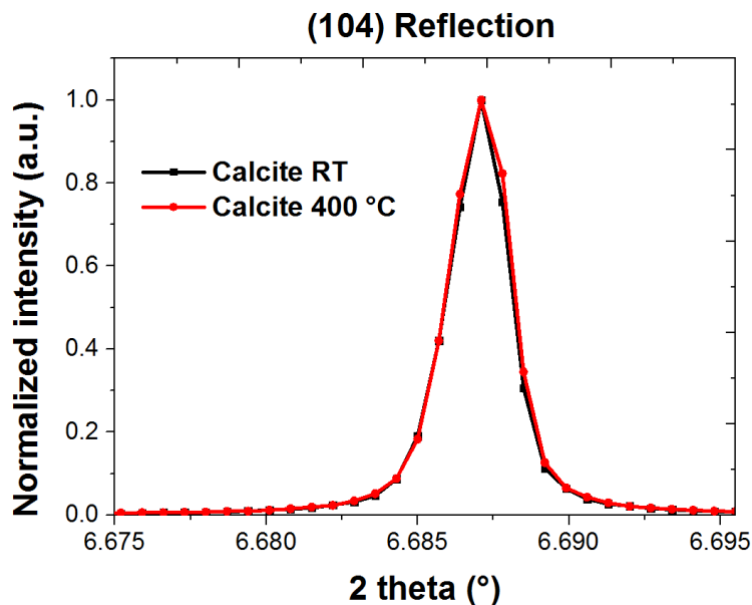

(104) Reflection

Figure 7. Diffractograms of the main (104) reflection of pure calcite at room temperature (black) and annealed at 400 °C for 2h.

Annealing of the Au/PEI-Calcite composites at 200 °C generated a very interesting behavior, where instead of observing typical lattice relaxations (*i.e.,* diffraction peaks returning to the same positions as those of the pure mineral), further lattice strain are observed (Figure 8). Indeed, a significant shift towards lower 2θ (*i.e.,* larger d-spacings) are observed. This is further pronounced for the composite crystals heated at a higher temperature, 400 °C, where the diffraction peaks are even more shifted towards lower 2θ, indicating further strain of the host crystals incorporating Au particles on annealing.
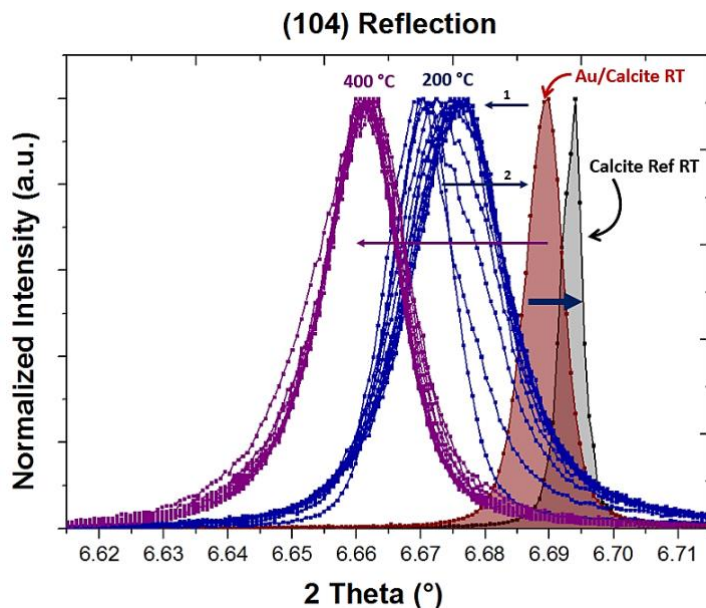
Figure 8. Diffractograms of the main (104) reflection of pure calcite (grey) and Au/PEI-Calcite (red) at room temperature and annealed at 200 °C (blue) and 400 °C (purple) for 2h.

Furthermore, lattice expansions were observed along the c-axis, while lattice contractions were recorded for the a-axis on annealing (Figure 9). The lattice distortions were greater along the c-axis than along the a-axis, consistent with the elastic anisotropy of calcite. That the lattice of calcite is further strained run counter previously reported data, where a lattice relaxation is typically observed.[1-5]
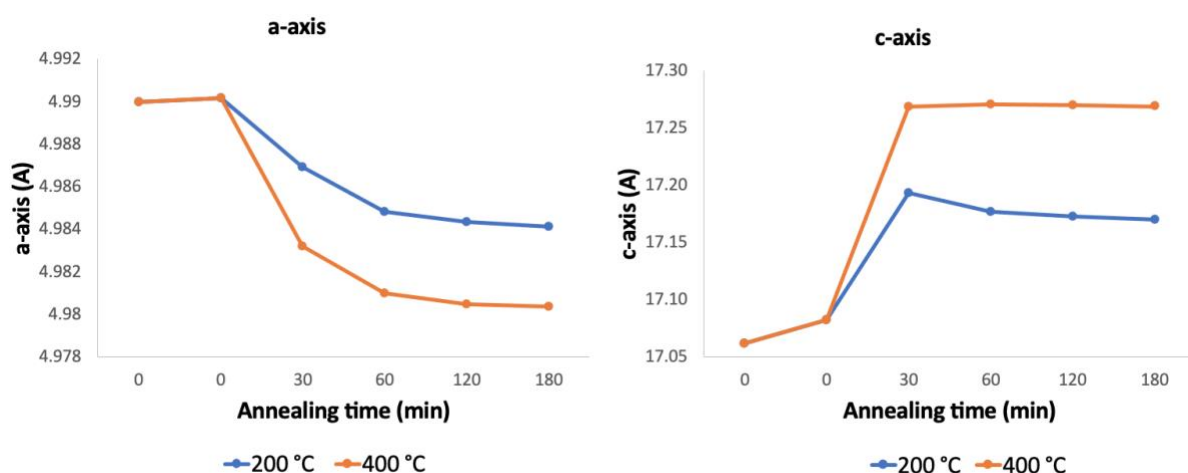

Figure 9. Evolution of the lattice parameters of Au/PEI-Calcite over time on annealing at 200 °C (blue) and 400 °C (orange).

That the Au/PEI-calcite composites behave oppositely to what is expected/reported in the literature is attributed to the annealing of the gold nanoparticles embedded within the calcite lattice. Indeed, looking at the main (111) and (200) reflections of the gold nanoparticles, we can see that the peaks become gradually sharper on annealing (Figure 10). At room temperature, only a hump is observed due to the very small size of the particle (*i.e.,* 5 nm Au-PEI particles).[4] With increasing heating temperature, an increase of the peak intensities and sharper diffraction peaks are recorded, indicative of the increase of crystallinity and size of the Au nanoparticles (Figure 10). Line profile analyses performed on the Au nanoparticles diffraction peaks indicate an increase of the crystallite size and a decrease of the lattice microstrain on annealing (Figure 11). Remarkably, it is also observed that the Au diffraction peaks tend to shift towards lower 2θ due to thermal expansion of the nanoparticles. This is coherent with the increase of the lattice parameter of the Au nanoparticles for the (111) main reflection when heated at 400 °C. Furthermore, microstrain fluctuations of the Au particles decreases considerably on heating, due to the thermal removal of grain boundaries.
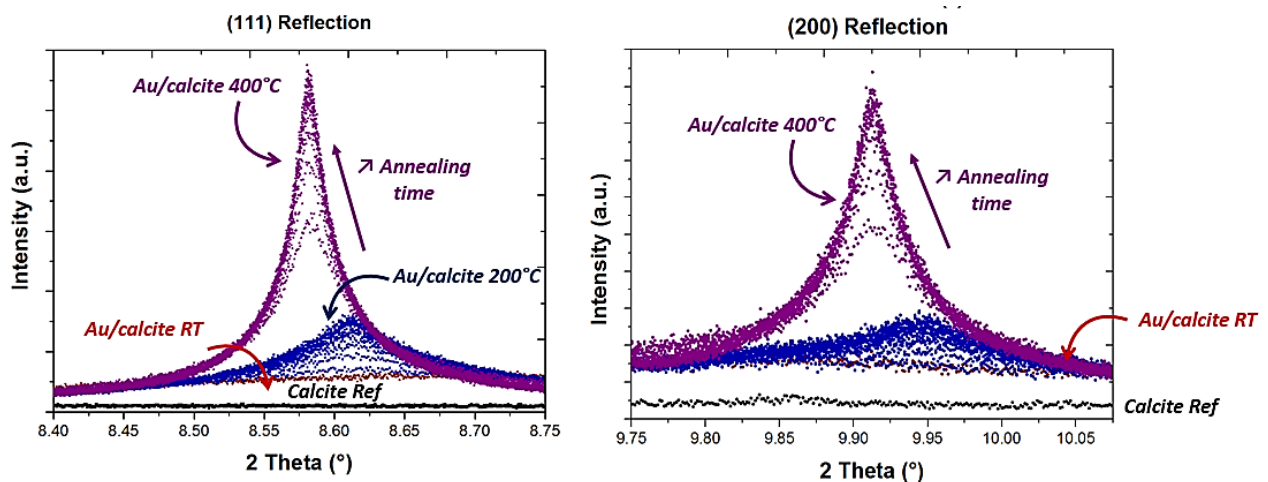

Figure 10. Diffractograms of evolution of the (111) and (200) main reflections of the Au nanoparticles on annealing over time.
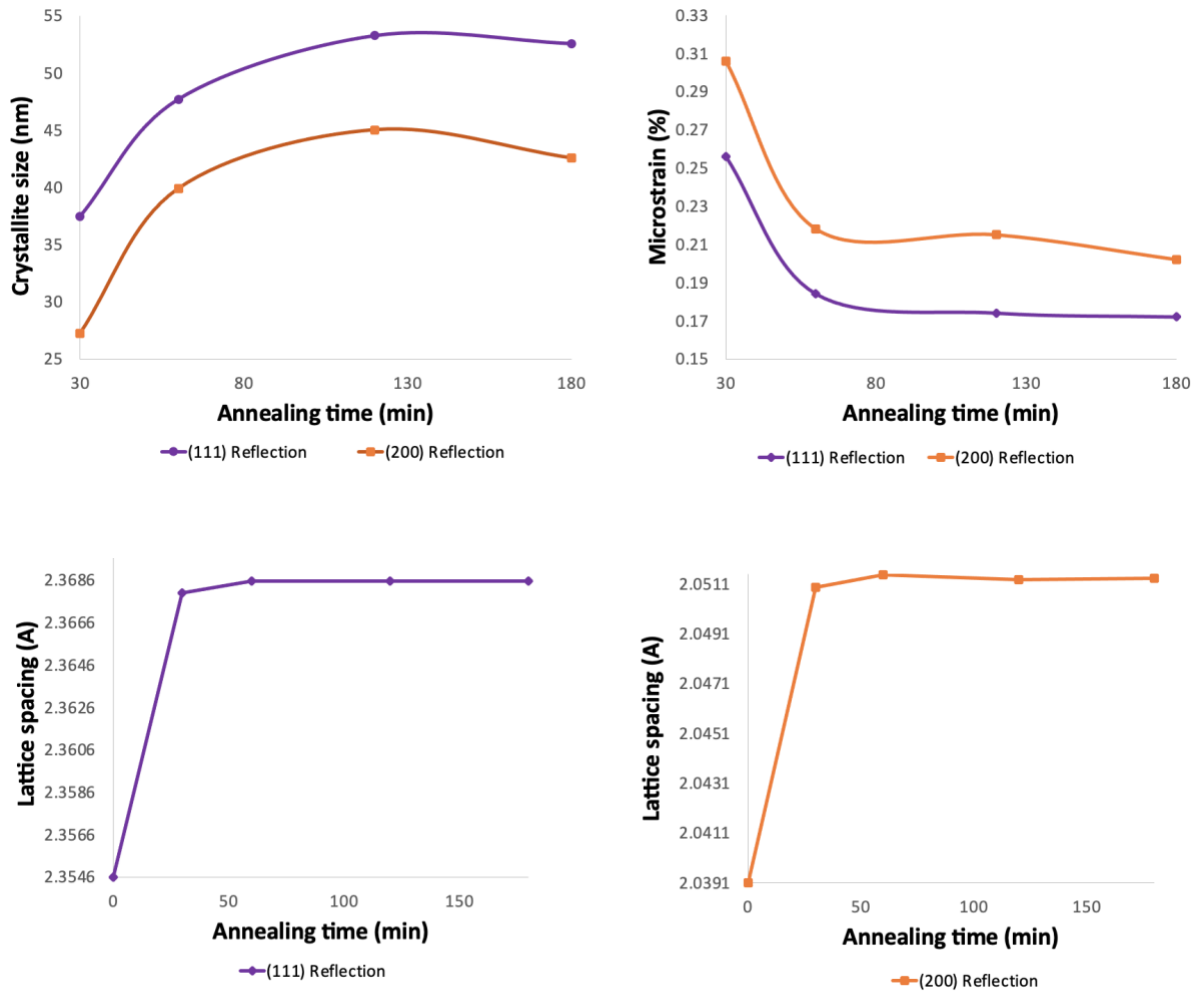
Figure 11. Evolution of the coherence lengths, microstrain fluctuations and lattice spacing of the (111) (purple) and (200) (orange) main reflections of the Au nanoparticles on annealing over time.

Taken together, these results are consistent with our Transmission Electron Microscopy (TEM) data, where we observed that annealing of the Au/calcite composite crystals enable *in-situ* growth of the Au nanoparticles within the host crystals from 5 nm to 40 nm in size (Figure 12).
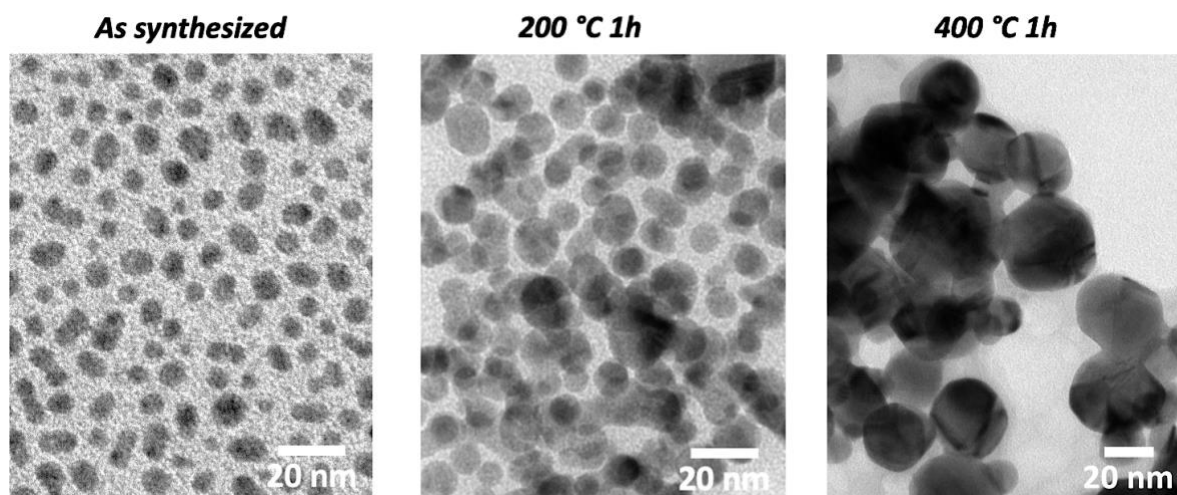
Figure 12. Transmission electron micrographs showing the increase of the size of the Au nanoparticles incorporated in calcite at room temperature and on annealing at 200 °C and 400 °C for 1 h.

c. Isochronous annealing of $MnCO_3$

Annealing of $Au/MnCO_3$ composites at 200 °C induced a unique behavior, where at the early stages of heating, a gradual shift of the diffraction peaks towards lower 2θ (corresponding to lattice relaxation) is observed (Figure 13). However, on prolonged annealing of the composites, the diffraction peaks of the host crystal shifted back towards higher 2θ (corresponding to lattice contraction). These results indicate that on annealing, the lattice strain of the host crystals first relaxes, followed by a gradual lattice strain/contraction. This is attributed to the thermal decomposition of the polymer during the early stages of annealing, followed by the *in situ* diffusion/movement and growth of the Au nanoparticles that induces further strain to the host crystals. This is also supported by the increase of intensity and shaper diffraction peaks of the main (111) Au peaks on annealing over time, which corresponds to an increase of size and crystallinity of the Au nanoparticles (Figure 13).

Note that annealing at higher temperatures (> 200 °C) induces phase transformation of rhodochrosite to manganese oxide. We did not explore higher annealing temperatures, as it would increase the degree of complexity of the systems, making analysis of the diffractograms and their interpretations more intricate.
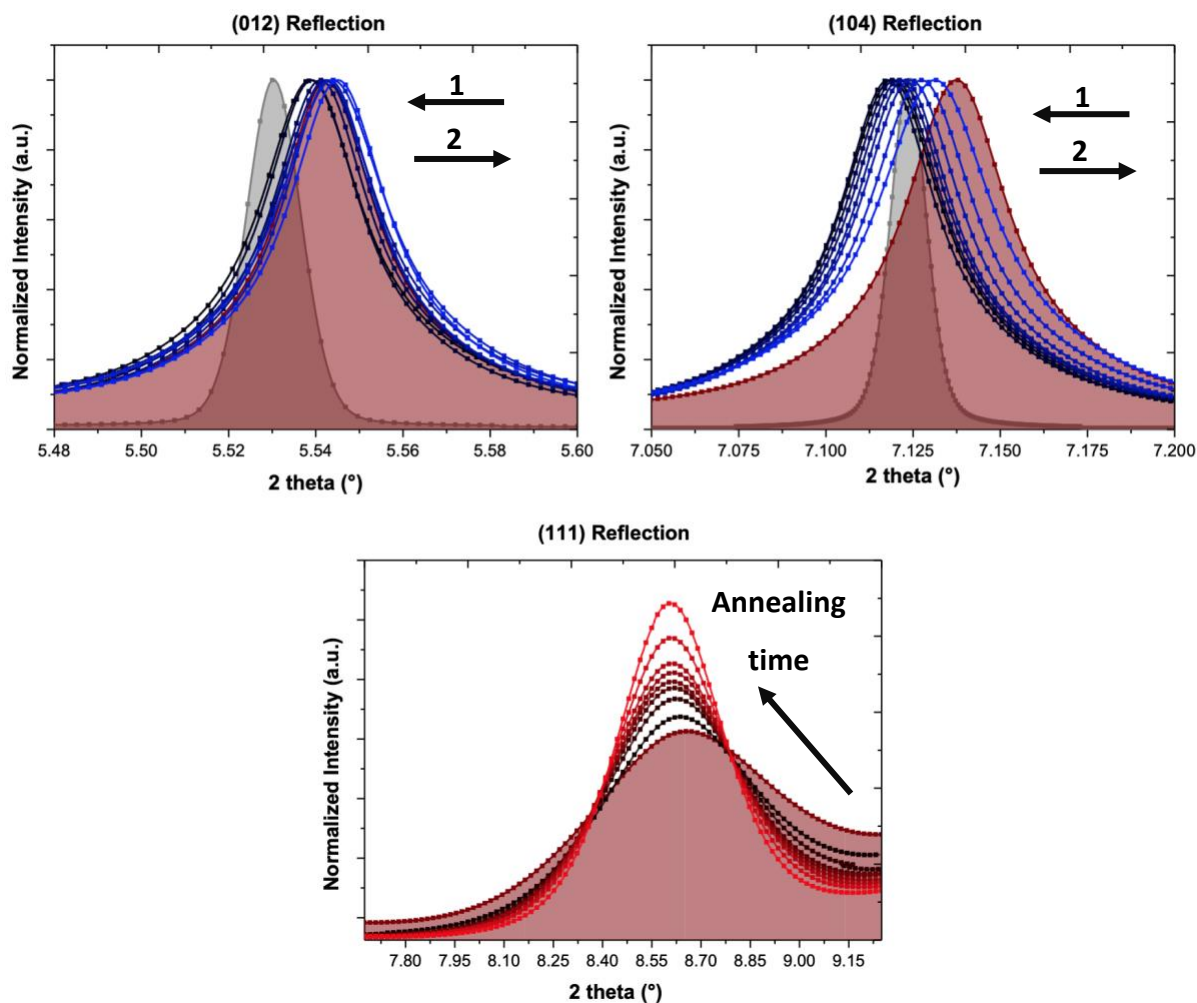
Figure 13. Evolution of the diffractograms of the main (012) and (104) reflections of pure MnCO$_3$ (grey) and Au/PEI-MnCO$_3$ (red) at room temperature and annealed at 200 °C over time. Bottom graph represents the evolution of the diffractograms of the main (111) reflection of the Au nanoparticles annealed over time.

d. Isochronous annealing of Au/ZnO composites

Similar to pure calcite, annealing of pure ZnO did not alter the crystal microstructure, where no changes of the peak shape, broadening or position were recorded for any of the zincite reflections (data not shown). This demonstrates that the pure crystals have a high purity level and therefore do not incorporate any impurities/organic matter within the mineral.

In contrast, isochronous annealing of Au/ZnO at 200 °C induced a shift of all diffraction peaks of ZnO host crystals towards lower 2θ, corresponding to lattice expansion (Figure 14). In addition, a broadening of all reflections is also observed, which corresponds to a decrease of

the coherence lengths in conjunction with an increase of the microstrain fluctuations. Interestingly, annealing of the Au/ZnO composites at 400 °C yielded similar results as annealing at 200 °C, where the diffraction peaks overlap.

Broadening of the peaks is most likely induced by the thermal decomposition of the polymer on the surface of the gold nanoparticles, while peaks shift results from the *in-situ* diffusion and growth of the Au nanoparticles that is thermally initiated.
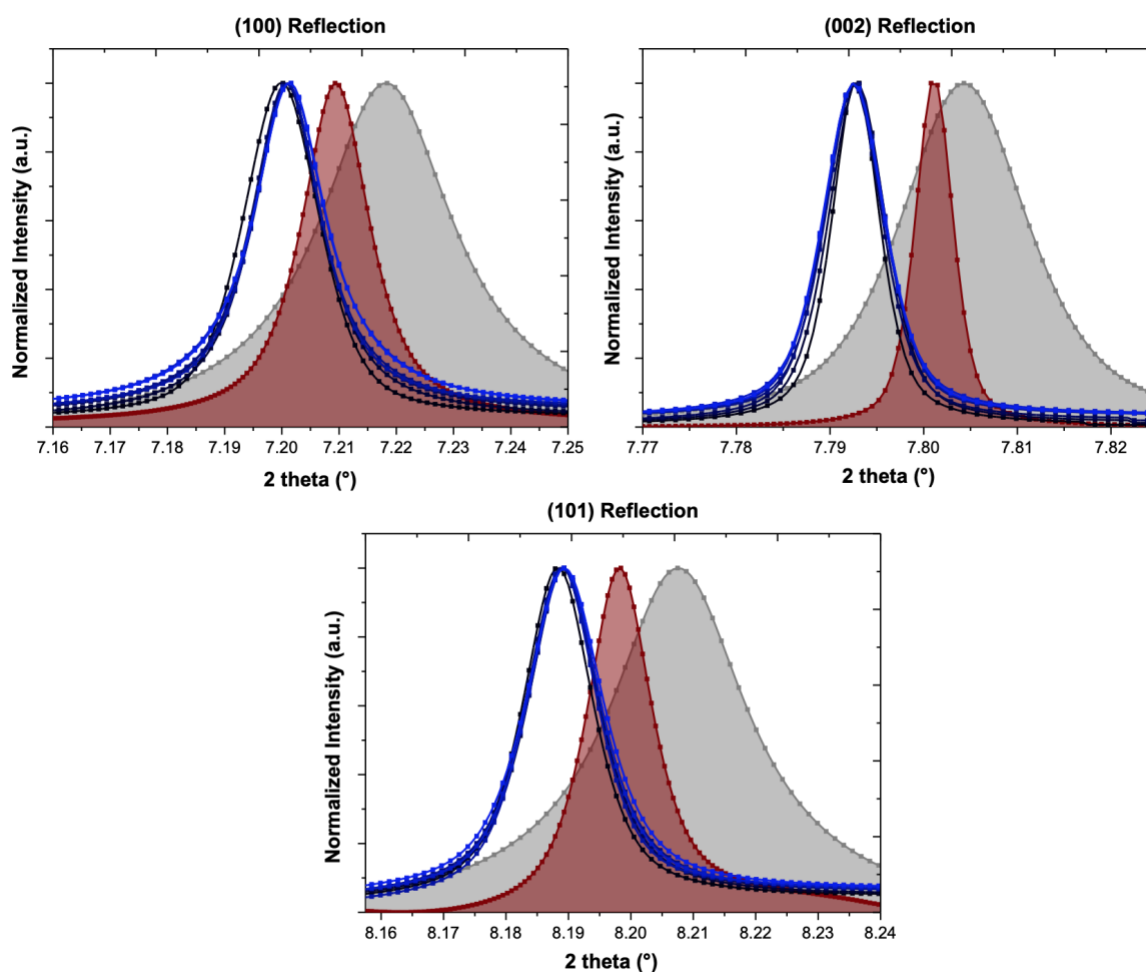

Figure 14. Evolution of the diffractograms of the main (100), (002) and (101) reflections of pure ZnO (grey) and Au/PEI-ZnO (red) at room temperature and annealed at 200 °C (blue) and 400 °C (black) over time.

4. Conclusions

We have carried out HR-PXRD of three composite materials incorporating high levels of Au nanoparticles. Room temperature data are showing very interesting results, where

depending on the host crystals, distinct behaviors are observed. Au incorporated in calcite and ZnO yielded considerable lattice expansions, while lattice contraction of $MnCO_3$ was observed. This is the first time that lattice contraction was observed on incorporating large amounts of particulate additives within single crystals. Annealing of the composite materials yielded even more interesting behaviors. Instead of the traditional lattice relaxation of the host crystals on annealing, which results from the thermal degradation of the polymer surrounding the Au nanoparticles, we observed even greater lattice expansions of the Au/Calcite and Au/ZnO host crystals. Au/$MnCO_3$ first relaxed on annealing and subsequently contracted back again on prolonged heating of the composites. We attribute these very interesting results to the diffusion/motion and growth of the gold nanoparticles within the lattice of the crystals. Indeed, structural analyses of the Au particles incorporated within the crystals also evolve on annealing, where sharper and more intense diffraction peaks were recorded. This indicates that the particles become larger over time when heated. This is possible only if the nanoparticles can diffuse, meet and rearrange themselves *in-situ* (*i.e.,* within the crystals). These data also complement nicely our on-going *in-situ* Transmission Electron Microscopy (TEM) and *ex-situ* Focused-Ion Beam (FIB) studies of the heating of these composite materials. Ultimately, this systematic study will provide crucial insights into the design of a new class of functional materials with tunable properties.

5. **Publications:** All HR-PXRD data collected will provide valuable information that will support our future publications.

6. **References**

1. Kim, Y.-Y.; Carloni, J. D.; Demarchi, B.; Sparks, D.; Reid, D. G.; Kunitake, Miki E.; Tang, C. C.; Duer, M. J.; Freeman, C. L.; Pokroy, B.; Penkman, K.; Harding, J. H.; Estroff, L. A.; Baker, S. P.; Meldrum, F. C., Tuning hardness in calcite by incorporation of amino acids. *Nature Materials* **2016,** 15, (8), 903-910.

2. Pokroy, B.; Fitch, A. N.; Lee, P. L.; Quintana, J. P.; Caspi, E. a. N.; Zolotoyabko, E., Anisotropic lattice distortions in the mollusk-made aragonite: A widespread phenomenon. *Journal of Structural Biology* **2006,** 153, (2), 145-150.

3.   Pokroy, B.; Fitch, A.; Zolotoyabko, E., The Microstructure of Biogenic Calcite: A View by High-Resolution Synchrotron Powder Diffraction. *Advanced Materials* **2006,** 18, 2363-2368.

4.   Kim, Y.-Y.; Darkins, R.; Broad, A.; Kulak, A. N.; Holden, M. A.; Nahi, O.; Armes, S. P.; Tang, C. C.; Thompson, R. F.; Marin, F.; Duffy, D. M.; Meldrum, F. C., Hydroxyl-rich macromolecules enable the bio-inspired synthesis of single crystal nanocomposites. *Nature Communications* **2019,** 10, (1), 5682.

5.   Zolotoyabko, E., Anisotropic Lattice Distortions in Biogenic Minerals Originated from Strong Atomic Interactions at Organic/Inorganic Interfaces. *Advanced Materials Interfaces* **2017,** 4, (1), 1600189.